HHS Public Access

Author manuscript

Mol Cell. Author manuscript; available in PMC 2018 November 29.

Published in final edited form as:

Mol Cell. 2018 March 01; 69(5): 866–878.e7. doi:10.1016/j.molcel.2018.02.002.

The ubiquitin E3/E4 ligase, UBE4A, fine-tunes protein ubiquitylation and accumulation at sites of DNA damage facilitating double-strand break repair

Keren Baranes-Bachar[1], **Adva Levy-Barda**[1], **Judith Oehler**[2], **Dylan A. Reid**[3], **Isabel Soria-Bretones**[4], **Ty C. Voss**[5], **Dudley Chung**[6], **Yoon Park**[7], **Chao Liu**[8], **Jong-Bok Yoon**[7], **Wei Li**[8], **Graham Dellaire**[6], **Tom Misteli**[5], **Pablo Huertas**[4], **Eli Rothenberg**[3], **Kristijan Ramadan**[2], **Yael Ziv**[1], and **Yosef Shiloh**[1,*]

[1]The David and Inez Myers Laboratory for Cancer Research, Department of Human Molecular Genetics and Biochemistry, Sackler School of Medicine, Tel Aviv University, Tel Aviv, 69978 Israel

[2]Cancer Research UK and Medical Research Council Oxford Institute for Radiation Oncology, Department of Oncology, University of Oxford, Oxford, UK

[3]Perlmutter NYU Cancer Center and Department of Biochemistry and Molecular Pharmacology, New York University School of Medicine, New York, NY 10016, USA

[4]Centro Andaluz de Biología Molecular y Medicina Regenerativa (CABIMER) and Department of Genetics, University of Sevilla, Sevilla, Spain

[5]National Cancer Institute, National Institutes of Health, Bethesda, MD 20892, USA

[6]Departments of Pathology and Biochemistry & Molecular Biology, Dalhousie University, Halifax, Nova Scotia, Canada B3H 4R2

[7]Department of Biochemistry and Protein Network Research Center, Yonsei University, 134 Shinchon-Dong, Seodaemoon-Gu, Seoul 120-749, Korea

[8]State Key Laboratory of Stem Cell and Reproductive Biology, Institute of Zoology, Chinese Academy of Sciences, Beijing 100101, PR China.

Summary

Double-strand breaks (DSBs) are critical DNA lesions that robustly activate the elaborate DNA damage response (DDR) network. We identified a critical player in DDR fine-tuning - the E3/E4 ubiquitin ligase, UBE4A. UBE4A's recruitment to sites of DNA damage is dependent on primary E3 ligases in the DDR and promotes enhancement and sustainment of K48- and K63-linked ubiquitin chains at these sites. This step is required for timely recruitment of the RAP80 and BRCA1 proteins and proper organization of RAP80- and BRCA1-associated protein complexes at DSB sites. This pathway is essential for optimal end-resection at DSBs, and its abrogation leads to up-regulation of the highly mutagenic alternative end-joining repair at the expense of error-free homologous recombination repair. Our data uncover a critical regulatory level in the DSB response

*Correspondence: Tel: +972 3 6409760; Fax: +972 3 6407471; yossih@post.tau.ac.il.

and underscore the importance of fine-tuning of the complex DDR network for accurate and balanced execution of DSB repair.

Keywords

genome stability; DNA damage; double-strand breaks; ubiquitin; UBE4A

Introduction

Maintenance of genome stability is critical for cellular homeostasis, streamlined development, and prevention of undue cell death, cancer and premature aging. A major axis in maintaining genome stability is the DNA damage response (DDR), a broad network that activates DNA repair mechanisms and sets in motion an elaborate series of events that swiftly modulate numerous physiological processes (Goldstein and Kastan, 2015; Sirbu and Cortez, 2013). The highly cytotoxic double-strand break (DSB) provokes a robust and highly coordinated response of the DDR network (Goldstein and Kastan, 2015; Goodarzi and Jeggo, 2013; Shiloh and Ziv, 2013a; Sirbu and Cortez, 2013).

DSBs are repaired mainly by end resection-independent, canonical nonhomologous end-joining (C-NHEJ), or resection-dependent homologous recombination repair (HRR) (Chang et al., 2017; Kowalczykowski, 2015). The predominant repair pathway is C-NHEJ, in which broken ends are processed and rejoined, operates throughout the cell cycle. HRR is based primarily on homologous recombination between the damaged DNA molecule and its intact sister, and therefore is active in the late S and G2 phases of the cell cycle. Minor resection-dependent pathways are single-strand annealing (SSA), and alternative NHEJ (alt-NHEJ) (also referred to as microhomology-mediated end joining) (Chang et al., 2017). These pathways are based on annealing of sequences of different lengths in the 3’ overhangs generated by 5’ end-resection (Symington, 2016). While HRR is error-free, the other pathways are variably error-prone. A delicate balance between these repair pathways is essential for orderly completion of DSB sealing, and its abrogation may retard DSB repair and enhance genome aberrations (Shibata and Jeggo, 2014). Many players in the DSB response relocate to DSB sites, where they form large protein hubs (Lukas et al., 2011). These proteins typically undergo post-translational modifications (PTMs), primarily poly(ADP-ribosylation), phosphorylation, and modification by the ubiquitin family proteins, which set them up to operate in the DDR (Harding and Greenberg, 2016; Lee et al., 2017; Martin-Hernandez et al., 2017; Polo and Jackson, 2011; Shiloh and Ziv, 2013a; Wilson and Durocher, 2017). This massive protein recruitment is a highly structured process, in which the damage-induced PTMs often establish interactions among the proteins to help mobilize and correctly locate the next-in-line recruits. Interference with this process usually leads to abrogation of DSB repair. The chief transducer of the signal emanating from the DSB sites is the protein kinase, ATM, which phosphorylates a plethora of substrates at these sites and elsewhere (Paull, 2015; Shiloh and Ziv, 2013b).

Protein ubiquitylation at DSB sites is carried out by several E3 ubiquitin ligases and is critical for mobilizing chromatin dynamics at these sites, appropriate recruitment of DDR

factors and, eventually, DSB repair (Harding and Greenberg, 2016; Lee et al., 2017). Indeed, extensive K48- and K63-linked ubiquitylations were observed at DSB sites (Lee et al., 2017; Meerang et al., 2011), but the number of documented ubiquitylation targets is limited and current consensual substrates are histones H2A, H2B and H1 (Harding and Greenberg, 2016; Lee et al., 2017). Identification of the ubiquitin ligases that take part in the DDR is key to understanding ubiquitin-driven pathways in this network. Major factors in H2A ubiquitylation are the E3 ligases, RNF8 and RNF168, whose activity is required for proper recruitment of the 53BP1 protein – a platform for additional DDR proteins and a regulator of DSB repair pathway choice – and RAP80, which anchors the protein complex, BRCA1-A, whose subsequent dynamics plays a role in the critical balance between DSB repair pathways (Lombardi et al., 2017).

Among the various families of E3 ubiquitin ligases, a small subgroup of the RING-type ligases contains a modified RING domain called U-box, which, like the RING domain, is essential for the enzyme's catalytic activity (Aravind and Koonin, 2000). One of the best characterized U-box ligases is the yeast protein, ubiquitin-fusion degradation 2 (Ufd2), which has been associated with endoplasmic-reticulum-associated protein degradation (ERAD) (Johnson et al., 1995). Ufd2 also possesses an E4 ligase activity. E3 ligases with E4 activity (E3/E4 ligases) can bind to a single conjugated ubiquitin or an oligoubiquitin chain generated by other E3 ligases and further extend and regulate the lengths of the chains (Hatakeyama et al., 2001; Hoppe, 2005). Ufd2 is conserved throughout evolution, with two orthologs in mammals that are likely paralogs, designated in humans UBE4A and UBE4B. UBE4B's E4 ligase activity has been demonstrated, and among its substrates are p53 and ataxin-3 (Du et al., 2015; Hatakeyama and Nakayama, 2003; Matsumoto et al., 2004; Park et al., 2008, 2009; Periz et al., 2015; Starita et al., 2013; Wu and Leng, 2011; Wu et al., 2011). UBE4A's activity and physiological significance have not been extensively documented. Recently it has been implicated in targeting interleukin-like EMT inducer for degradation (Sun et al., 2017).

Here, we show that UBE4A is a critical DDR factor. It has an E4 ubiquitin ligase activity *in vitro*, and in cells its presence is required for tweaking the extent of both K48- and K63-linked ubiquitin chains at sites of DNA damage. Acting downstream of the primary E3 ligases in the DDR and 53BP1, UBE4A's action in fine adjustment of ubiquitin chain length is required for proper internal organization of DSB-associated protein foci, and ultimately for maintaining the exquisite balanced between DSB repair pathways and timely DSB repair.

Results

UBE4A is essential for appropriate cellular response to DSBs

Our attention was drawn to UBE4A and UBE4B when UBE4B was identified as a hit in a functional screen we carried out in search of novel determinants of ubiquitylation in the DDR (Figure S1 and Supplemental Information). In view of their sequence similarity, we explored the possibility that both proteins are involved in the DDR. Initial experiments indicated that this was the case, but UBE4A and UBE4B seemed to function separately in different DDR branches. Here, we focus on UBE4A, the less studied paralog (Figure 1A). First indication that UBE4A functions in the DSB response came from the observation that

its depletion led to cellular hypersensitivity to the radiomimetic drug, neocarzinostatin (NCS), in a clonogenic survival assay (Figure 1B). Such sensitivity is suggestive of defective DSB repair. In order to directly examine the effect of UBE4A depletion on DSB sealing, we used the sensitive neutral comet assay (Glei et al., 2016) to measure the amount of DSBs remaining in genomic DNA after treatment with ionizing radiation (IR). Significant differences in comet tail moment (an actual measure of DSBs in the neutral comet assay) were observed between UBE4A-proficient and -depleted cells 24 hr after IR treatment (Figure 1C), indicating a marked, continuous retardation in DSB closure upon reduction of UBE4A level. Similarly, UBE4A depletion led to retarded disappearance of nuclear foci of the DDR protein, 53BP1, 24 hr after treatment with NCS (Figure 1D). Importantly, ectopic expression of wild-type UBE4A in cells depleted of the endogenous protein complemented the defective repair phenotype, while a potentially inactive mutant protein lacking the U-box failed to do so (Figure 1D), suggesting that the catalytic activity of UBE4A is essential for its function in DSB repair.

UBE4A is recruited to sites of DNA damage, dependent upon major E3 ligases in the DDR, and 53BP1

A common attribute of many DSB response players is their temporary relocation to the damage sites. In view of the above results we asked whether UBE4A undergoes such relocation. The dynamics of this recruitment is usually monitored after induction of localized DNA damage in a narrow nuclear sector using a focused laser microbeam. We observed relocalization to such “laser stripes” of a portion of ectopic, GFP-tagged UBE4A within minutes of damage induction (Figure 2A). Mutant protein lacking the U-box was recruited at similar kinetics (Figure 2A), indicating that UBE4A’s catalytic activity was not required for this process. We further demonstrated UBE4A’s recruitment to damage sites by following the relocation of endogenous UBE4A to ‘laser stripes’, using a specific antibody (Figure 2B). The data thus establish that UBE4A is part of the large cohort of proteins that function at DSB sites and are required for efficient DSB repair.

The formation of the protein hubs spanning DSBs is a structured, hierarchical process, and the precise order of protein relocalization to the break sites reflects the dependence of each protein’s recruitment on previously recruited ones. In order to place UBE4A in this hierarchy, we examined the dependence of its recruitment on selected proteins in the cascade. Out of this list, depletion of 53BP1 and the E3 ubiquitin ligases, RNF8 and RNF168, markedly affected UBE4A recruitment, and depletion of the E3 ligase, RNF4, moderately reduced it (Figures 2C, S2A, B). These E3 ligases drive a major ubiquitylation cascade at DSB sites that is essential for DSB repair. Thus, our results suggest that timely appearance of UBE4A at the damage sites depends on prior protein ubiquitylation at these sites, and on prior presence at these sites of 53BP1 – a central regulator of the choice between DSB repair pathways (Daley and Sung, 2014; Gupta et al., 2014).

The yeast ortholog of UBE4A and UBE4B – Ufd2 – functions in close collaboration and physical association with the ATPase, Cdc48, and with the Rad23 protein (Baek et al., 2013). The human ortholog of Cdc48, p97/VCP, was recently reported to play a role in the DSB response (Torrecilla et al., 2017). The mammalian paralogs of Rad23, RAD23A and

RAD23B are involved in the response to bulky DNA lesions via the nucleotide excision repair pathway (Yokoi and Hanaoka, 2017). We therefore examined the possible dependence of UBE4A's recruitment to damage sites on these proteins. We found that RAD23A, RAD23B and VCP were not required for UBE4A recruitment to damage sites; nor was UBE4A's paralog, UBE4B, necessary for this process (Figures 2C, S2A, C). Furthermore, depletion of UBE4A did not affect the recruitment of the DDR proteins, RNF8, RNF168, 53BP1, and MDC1, or γH2AX formation (Figure S2D). These experiments place UBE4A at a relatively late stage in the hierarchy of protein assembly at DSB sites, with dependence on prior protein ubiquitylation within these protein assemblies and downstream of 53BP1. Interestingly, we found that UBE4A co-immunoprecipitates with 53BP1 and this co-immunoprecipitation is enhanced by DNA damage (Figure S3). This observation and the 53BP1 dependence of UBE4A recruitment suggest that UBE4A's entry into the DSB response cascade is mediated at least in part by direct or indirect interaction with 53BP1.

UBE4A activity and UBE4A-dependent modulation of K48- and K63-linked ubiquitin chains at damage sites

We assumed that UBE4A functions at DSB sites in its capacity as an E4 ubiquitin ligase, an activity that was previously demonstrated in its paralog, UBE4B. In order to demonstrate UBE4A's E4 activity, we carried out an experiment similar to a previous one that showed UBE4B's E4 activity *in vitro* (Park et al., 2009). The UFD pathway can be probed in cells and *in vitro* using an artificial substrate, monoubiquitylated GFP (Dantuma et al., 2000). Using such substrate, in which the ubiquitin moiety is mutated and thus uncleavable (Ub^{G76V}), the Yoon lab previously found that the HECT domain E3 ligase, TRIP12, functions in the UFD pathway in mammalian cells, but for optimal ubiquitylation of the substrate, TRIP12's activity should be followed by the E4 activity of UBE4B (Park et al., 2009). This requirement for both the E3 and E4 ligases for optimal substrate ubiquitylation was demonstrated *in vitro* (Park et al., 2009). In an analogous experiment we used the same *in vitro* system, only with UBE4A as the E4 ligase (Figures 3, S4). We found that, similarly to its paralog, UBE4B (Park et al., 2009), UBE4A functions in this reaction as an E4 ligase. Further evidence for UBE4A's involvement in protein ubiquitylation *in cells* was obtained by examining the effect of its depletion on cellular protein ubiquitylation using a method developed recently to pull down ubiquitylated proteins from cellular extracts (Sims et al., 2012). According to this method, ubiquitin-interacting domains (UIMs) are expressed in cells and are subsequently immunoprecipitated using an attached tag that pulls down interacting proteins. We used a construct containing 3 tandem UIMs derived from the DDR protein, RAP80, which selectively bind K63-linked ubiquitin chains (Sims et al., 2012; Thorslund et al., 2015). Indeed, UBE4A depletion decreased the amount of K63-linked ubiquitylation in unirradiated and X-irradiated cells (Figure S5), suggesting a role for UBE4A in shaping protein ubiquitylation in cells in several ubiquitin-driven processes, similarly to its paralog UBE4B.

The E4 ligase function is plausibly broad and used in various physiological contexts. Accordingly, E3/E4 ligases have broad specificity with regard to the types of ubiquitin chains they extend, which may depend on the combinations of E2 and E3 ligases in specific reactions (Ackermann et al., 2016; Hatakeyama and Nakayama, 2003; Hoppe, 2005; Liu et

al., 2017; Matsumoto et al., 2004; Park et al., 2008, 2009; Saeki et al., 2004; Wu and Leng, 2011; Wu et al., 2011). UBE4B was shown to extend K27-, K33- and K48-linked chains (Hatakeyama and Nakayama, 2003; Hatakeyama et al., 2001; Park et al., 2008, 2009; Wu and Leng, 2011; Wu et al., 2011). Yeast Ufd2 catalyzes the extension of K29- and K48-linked chains (Ackermann et al., 2016; Saeki et al., 2004) and creates branched chains by catalyzing K48-linked multi-monoubiquitylation on K29-linked ubiquitin chains (Liu et al., 2017). *C. elegans* Ufd-2 extends K29- and K48-linked chains (Ackermann et al., 2016) as well as K63-linked chains (Wojtek Pokrzywa and Thorsten Hoppe, unpublished). DSB sites are characterized by extensive K48- and K63-linked protein ubiquitylation (Meerang et al., 2011; Ramadan, 2012). We asked whether UBE4A was involved in extending these chain types at sites of DNA damage. Previous work showed that K48-linked ubiquitylation at damage sites mounts rapidly, peaks 15 min after damage induction, and decreases sharply within the next hour, while K63-linked ubiquitylation peaks 1 hr after damage induction and persists for several hours (Meerang et al., 2011; Ramadan, 2012). These experiments were based on quantitating the signal obtained at laser stripes after immunostaining with antibodies specific for these ubiquitin chain types. Cells depleted for the p97/VCP protein serve as controls in these experiments, since loss of this protein leads to excessive accumulation of ubiquitylated proteins at damage sites (Meerang et al., 2011).

We quantified the average intensity of K48- and K63-linked ubiquitylation at DNA damage sites using antibodies specific for these chain types (Figure S6). UBE4A depletion markedly decreased but did not eliminate the average K48 signal 15 min after damage induction, and the effect was diminished 2 hr later, when the K48 signal usually subsided (Figures 4A, B, S7A). When we classified the ubiquitin signals as ‘strong’, ‘average’ and ‘undetectable’ (Figure S7B), cells depleted of UBE4A had a significantly lower fraction of ‘strong’ K48 stripes and higher fraction of ‘undetectable’ stripes 15 min after damage induction, compared to siCTRL-treated cells (Figure 4C). This implies that UBE4A is important for timely formation of K48-linked ubiquitin chains in proper amounts at the sites of DNA damage. Quantifying the intensity of K63-linked chains at the sites of DNA damage showed that depletion of UBE4A led to lower average intensity of these chains relative to the control, both 15 min and 2 hr after induction of DNA damage (Figures 4D, E, S7C). Accordingly, UBE4A depletion led to a markedly higher fraction of cells with undetectable K63-linked chain signals at damage sites compared to siCTRL, and a lower fraction of average and strong intensity chain signals (Figure 4F). Taken together, these data establish that UBE4A is critical for the required timing and amount of two major types of ubiquitylation that occur ubiquitously at sites of DNA damage: K48-linked ubiquitylation, which marks target proteins for proteasome-mediated degradation, and K63-linked chains, which alter protein function or mode of action (Spasser and Brik, 2012; Williamson et al., 2013).

UBE4A is required for complete assembly of specific DDR factors at DSB sites and proper internal organization of DSB-associated protein foci

An important outcome of K63-linked ubiquitylation at DSB sites is the recruitment of the DDR factors, RAP80, which has specific affinity to these ubiquitin chains due to its tandem ubiquitin-interacting motifs (Lombardi et al., 2017). Indeed, UBE4A depletion led to

reduced accrual of RAP80 at DNA breaks (Figure 5A) in a manner that was dependent on UBE4A activity (Figure 5B). A further consequence of UBE4A depletion was reduced recruitment of BRCA1, which is dependent on RAP80 (Figure 5C). RAP80 recruitment was not completely abolished, however, since UBE4A depletion does not completely eliminate protein ubiquitylation at damage sites (Figure 4). Further downstream is the major HRR protein, RAD51, and here too damaged UBE4A-depleted cells exhibited a significantly lower number of nuclear RAD51 foci at the S and G2 cell cycle phases (in which HRR functions) (Figure 5D).

Once these proteins are recruited to DSB sites their precise assembly there in space and time and the dynamics of the internal focus organization are critical for proper DSB repair (Lukas et al., 2011). In order to study this organization we used single-molecule localization-based super-resolution (SR) imaging, a powerful form of fluorescent microscopy that offers a ten-fold improvement over conventional diffraction-limited microscopy, such as confocal microscopy (Huang et al., 2009). The modality was recently used to examine the organization of DSB repair proteins at damage sites (Conlin et al., 2017; Reid et al., 2015) (See Figures 6A, B for examples). To generate SR images, we used direct Stochastic Optical Reconstruction Microscopy (dSTORM) to localize single-fluorescent dye molecules below the diffraction limit (van de Linde et al., 2011). In dSTORM, fluorescent dyes are predominately in a dark state (not fluorescing) due to the presence of the chemical mercaptoethylamine (MEA). However, at any given time a small, sparse, subset of fluorophores emits fluorescence, permitting their localization. This population changes stochastically, and by acquiring a series of images from a viewing field, a super-resolved image can be generated with coordinates of each localized molecule. The Rothenberg and other groups recently used this approach to study the structure of DNA damage-associated protein foci (Britton et al., 2013; Doksani et al., 2013; Reid et al., 2015; Young et al., 2015), as well as other systems that challenge imaging due to a size that is close to the diffraction limit, such as neuronal synapses (Dani et al., 2010). Moreover, since single dyes are localized, this technique is substantially more sensitive than other super-resolution techniques so analysis is not necessarily confined to the brightest foci. Here, the information obtained allows us to make quantitative determinations, such as the area occupied by various proteins (Wani et al., 2016) that might be missed with conventional imaging. In addition we can measure the degree of overlap between proteins (Figures 6A, B) yielding information about the spatial organization and physical proximity among proteins within the focus. These parameters may point to the intactness of the processes in which these protein function. Since UBE4A depletion affected the recruitment of RAP80, BRCA1, and RAD51 (Figure 5), we focused on these proteins as well as two other HRR factors, BRCA2 and PALB2.

RAP80 mediates the recruitment of the BRCA1-A complex, which includes BRCA1, RAP80, ABRAXAS, and MERIT40 and antagonizes HRR (Coleman and Greenberg, 2011). This barrier to HRR is subsequently removed during spreading and repositioning of the BRCA1-A complex and the formation of the BRCC complex, which includes BRCA1, BRCA2, PALB2 and RAD51 and drives HRR [reviewed by (Park et al., 2014)]. Notably, the spatial distribution of RAP80 foci determined here using dSTORM (~0.3-0.4 micron^2; Fig. S8) was similar to that previously reported using correlative light and electron microscopic

imaging of γH2AX foci (Dellaire et al., 2009). We also found that, compared to controls, the areas occupied by RAP80 and BRCA1 were larger in UBE4A-depleted cells at early time points (5-30 min after damage induction), and returned to normal values 6 hr later (Figures 6C-E, S8A, B). On the other hand, the areas occupied by BRCA2 and PALB2 after UBE4A depletion were smaller than in control cells (Figure 6C). Accordingly, UBE4A depletion led to increased overlaps of RAP80 and BRCA1 with γH2AX, and decreased these overlaps for BRCA2, PALB2 and RAD51 (Figures 6D, E). The results suggested that UBE4A depletion caused increased presence of the BRCA1-A complex and reduced presence of the BRCC complex at the early time points after DSB induction, which could lead a-priori to reduced HRR. Taken together, the results show that the recruitment of UBE4A downstream of 53BP1 and its E4 ligase activity are required for shaping up the protein ubiquitylation at DSB sites essential to optimal buildup of the protein array required for HRR (Figure 6F). We therefore proceeded to examine the interplay between DSB repair pathways upon UBE4A depletion.

A shift from HRR to alt-NHEJ upon UBE4A depletion

HRR – the only error-free pathway – was evaluated in UBE4A-depleted cells using two different assays. The extensively documented DR-GFP reporter provides a fluorescent readout of HRR that takes place at a break induced by the restriction enzyme I-SceI (Pierce et al., 2001). This assay showed moderate reduction in HRR upon UBE4A depletion (Figure 7A). A recently developed system for measuring the efficiency of homology-directed repair (HDR) is the CRISPR-LMNA HDR assay (Pinder et al., 2015) (Figure S9). In this assay, a Cas9-generated DSB at the *LMNA* gene locus is repaired using a DNA homology donor encoding the green fluorescent protein, Clover, flanked by homology to the endogenous *LMNA* locus. Successful HDR between the homology donor and the *LMNA* locus results in expression of Clover-tagged LMNA and green fluorescence at the nuclear lamina. Depletion of UBE4A significantly reduced the efficiency of CRISPR-mediated HDR, by 40% compared to an irrelevant siRNA, whereas a 70% reduction in HDR was conferred by depletion of a major HRR factor, RAD51 (Figure 7B). In parallel, we measured the effect of UBE4A depletion on C-NHEJ, alt-NHEJ and SSA, as well as the extent of end-resection at DSBs. Importantly, while C-NHEJ and SSA were not affected, alt-NHEJ was increased in UBE4A-depleted cells (Figures 7C-E). End-resection – a key apical process in the decision among DSB repair pathways – was moderately reduced upon UBE4A depletion (Figure 7F). These results suggest that, following UBE4A depletion, end-resection becomes suboptimal and resection intermediates that cannot serve as HRR starting points are channeled to the highly error-prone alt-NHEJ (Figure 7G). Such shift in the balance between repair pathways is also likely to leave unrepaired breaks (Figure 1C). Thus, the UBE4A-dependent pathway culminates in the exquisite regulation of the balance among DSB repair pathways.

Discussion

The DSB response is an intricate, multi-level operation, and the activity within the massive protein hubs that form around DSBs attests to a highly complex cascade of events. Despite the complexity, this is a fine-tuned process that brings each DDR protein to the protein conglomerates spanning DSB sites at the precise time and location to perform the ultimate

task: smooth and streamlined DSB repair. The importance of tight regulation of protein ubiquitylation in this process has been noted (Harding and Greenberg, 2016; Lee et al., 2017; Panier and Durocher, 2013). A primary level of this regulation is the universal balance between the relevant E3 ligases and opposing deubiquitylating proteases (DUBs) (Pellegrino and Altmeyer, 2016). Interestingly, the DUBs USP26 and USP27 were found to modulate RNF168-mediated protein ubiquitylation at DSB sites thereby preventing excessive spreading of RAP80-BRCA1, promoting association of BRCA1 with PALB2 and streamlining HRR (Typas et al., 2015), similarly to the role we attribute to UBE4A. Another level of regulation is mediated by opposing actions of E3 ligases. The E3 ligase, RNF169, was found to be recruited to DSB sites in an RNF8/RNF168-dependent manner and attenuate ubiquitin-mediated signaling and accumulation of 53BP1 and RAP80 at damaged chromatin, thereby stimulating HRR and restraining NHEJ (Chen et al., 2012; Poulsen et al., 2012). RNF168 recruitment itself was found to be modulated by two other E3 ligases, TRIP12 and UBR5 (Gudjonsson et al., 2012).

Here, we add another control layer to this cascade: the careful regulation of the extent of protein ubiquitylation at the damage sites by an E3/E4 ubiquitin ligase, UBE4A. Recently, (Ackermann et al., 2016) reported that in *C. elegans* UFD-2 was involved in the DDR in the worm's gonad, in a different capacity than that of UBE4A's role in the DSB response reported here. In that organism, the E3/E4 ligase plays a role in the decision between cell survival and apoptosis following induction of DNA damage. Despite the different pathways, the work of Ackerman et al. (2016) and our data indicate that meticulous shaping of ubiquitin chains by an E3/E4 ligase is essential for proper DDR throughout evolution.

Our mechanistic insight into the actual role of UBE4A-mediated ubiquitylation highlights the tight regulation of the balance between DSB repair pathways. Our data demonstrate that this fine-tuned regulatory system is abrogated in the absence of UBE4A, as a result of improper accumulation and organization at DSB sites of its components. This ultimately leads on one hand to retarded formation of the BRCC complex that is necessary for HRR, and on the other hand – to incomplete end-resection at DSB sites – another critical step in the HRR pathway. Subsequently, the resection intermediates are used by the highly error-prone alt-NHEJ pathway, rather than the error-free HRR (Figure 7G). Both HRR and alt-NHEJ rely on end-resection, and the extent of this critical step in DSB repair is subject to stringent regulation (Symington, 2016). Because HRR requires longer single-stranded 3' overhangs, it is plausible that insufficiently resected overhangs will serve as alt-NHEJ substrates. Indeed, HRR deficiency due to deletions of RAD51 or RAD52 in yeast elevates alt-NHEJ (also called MMEJ) (Deng et al., 2014; Villarreal et al., 2012), and alt-NHEJ is elevated in human cells following BRCA1 elimination (Yun and Hiom, 2009).

The emerging picture is one of successive action of E3 ligases followed by an E3/E4 ligase, collectively shaping carefully and meticulously the ubiquitylation landscape around the break site. The exact sculpting of this landscape is essential for accurate protein dynamics and subsequent DSB repair. This process is intolerant of even the slightest perturbation, which can cause delayed or aberrant DSB repair, either of which may result in genomic rearrangements. The sophisticated regulation of the DDR and the absolute requirement of

every last one of its components explain why mutations that affect any one of them can lead to grave phenotypic outcomes.

Supplementary Material

Refer to Web version on PubMed Central for supplementary material.

Acknowledgments

We thank Kay Hofmann for valuable help with designing the siRNA libraries for the high-throughput screen, Thanos Halazonetis for anti-53BP1 antibody, Ron Hay for anti-RNF4 antibody, Daniel Durocher for FLAG-53BP1 construct, Niels Mailand for the K63-UIM construct and technical advice, and Ron Jachimowicz for critical reading of the manuscript. Work in YS laboratory is funded by research grants from the Dr. Miriam and Sheldon G. Adelson Medical Research Foundation, The A-T Children's Project, The Israel Science Foundation joint ISF-NSFC Research Program (jointly funded by the Israel Science Foundation and the National Natural Science Foundation of China), and The Israel Cancer Research Fund. The TM lab was supported in part by the Intramural Research Program of the National Institutes of Health, National Cancer Institute Center for Cancer Research. Work in the KR laboratory is supported by The Swiss National Science Foundation and The Medical Research Council, UK. Work in the GD laboratory is supported by a Discovery Grant from the Natural Sciences and Engineering Research Council of Canada (NSERC) (RGPIN 05616). Work in the PH lab was supported by R+D+I grant from the Spanish Ministry of Economy and Competitivity (SAF2013-43255-P) and an ERC Starting Grant (DSBRECA). Work in the ER laboratory is supported by National Institutes of Health Grants GM057691, CA187612, and the American Cancer Society grant ACS130304-RSG-16-241-01-DMC. IS-B is the recipient of a PhD fellowship from the University of Sevilla. DC was supported by the Nova Scotia Graduate Scholarship. KBB is a Jack and Florence Berlin Fellow. YS is a Research Professor of the Israel Cancer Research Fund.

References

Ackermann L, Schell M, Pokrzywa W, Kevei E, Gartner A, Schumacher B, and Hoppe T (2016). E4 ligase-specific ubiquitination hubs coordinate DNA double-strand-break repair and apoptosis. Nat Struct Mol Biol 23, 995–1002. [PubMed: 27669035]

Aravind L, and Koonin EV (2000). The U box is a modified RING finger - a common domain in ubiquitination. Curr Biol 10, R132–134. [PubMed: 10704423]

Baek GH, Cheng H, Choe V, Bao X, Shao J, Luo S, and Rao H (2013). Cdc48: a swiss army knife of cell biology. J Amino Acids 2013, 183421. [PubMed: 24167726]

Bennardo N, Cheng A, Huang N, and Stark JM (2008). Alternative-NHEJ is a mechanistically distinct pathway of mammalian chromosome break repair. PLoS Genet 4, e1000110. [PubMed: 18584027]

Britton S, Coates J, and Jackson SP (2013). A new method for high-resolution imaging of Ku foci to decipher mechanisms of DNA double-strand break repair. J Cell Biol 202, 579–595. [PubMed: 23897892]

Chang HHY, Pannunzio NR, Adachi N, and Lieber MR (2017). Non-homologous DNA end joining and alternative pathways to double-strand break repair. Nat Rev Mol Cell Biol 18, 495–506. [PubMed: 28512351]

Chen J, Feng W, Jiang J, Deng Y, and Huen MS (2012). Ring finger protein RNF169 antagonizes the ubiquitin-dependent signaling cascade at sites of DNA damage. The Journal of biological chemistry 287, 27715–27722. [PubMed: 22733822]

Coleman KA, and Greenberg RA (2011). The BRCA1-RAP80 complex regulates DNA repair mechanism utilization by restricting end resection. J Biol Chem 286, 13669–13680. [PubMed: 21335604]

Conlin MP, Reid DA, Small GW, Chang HH, Watanabe G, Lieber MR, Ramsden DA, and Rothenberg E (2017). DNA Ligase IV Guides End-Processing Choice during Nonhomologous End Joining. Cell Rep 20, 2810–2819. [PubMed: 28930678]

Cruz-Garcia A, Lopez-Saavedra A, and Huertas P (2014). BRCA1 accelerates CtIP-mediated DNA-end resection. Cell Rep 9, 451–459. [PubMed: 25310973]

Daley JM, and Sung P (2014). 53BP1, BRCA1, and the choice between recombination and end joining at DNA double-strand breaks. Molecular and cellular biology 34, 1380–1388. [PubMed: 24469398]

Dani A, Huang B, Bergan J, Dulac C, and Zhuang X (2010). Superresolution imaging of chemical synapses in the brain. Neuron 68, 843–856. [PubMed: 21144999]

Dantuma NP, Lindsten K, Glas R, Jellne M, and Masucci MG (2000). Short-lived green fluorescent proteins for quantifying ubiquitin/proteasome-dependent proteolysis in living cells. Nat Biotechnol 18, 538–543. [PubMed: 10802622]

Dellaire G, Kepkay R, and Bazett-Jones DP (2009). High resolution imaging of changes in the structure and spatial organization of chromatin, gamma-H2A.X and the MRN complex within etoposide-induced DNA repair foci. Cell Cycle 8, 3750–3769. [PubMed: 19855159]

Deng SK, Gibb B, de Almeida MJ, Greene EC, and Symington LS (2014). RPA antagonizes microhomology-mediated repair of DNA double-strand breaks. Nat Struct Mol Biol 21, 405–412. [PubMed: 24608368]

Doksani Y, Wu JY, de Lange T, and Zhuang X (2013). Super-resolution fluorescence imaging of telomeres reveals TRF2-dependent T-loop formation. Cell 155, 345–356. [PubMed: 24120135]

Du C, Wu H, and Leng RP (2015). UBE4B targets phosphorylated p53 at serines 15 and 392 for degradation. Oncotarget.

Glei M, Schneider T, and Schlormann W (2016). Comet assay: an essential tool in toxicological research. Arch Toxicol 90, 2315–2336. [PubMed: 27378090]

Goldstein M, and Kastan MB (2015). The DNA damage response: implications for tumor responses to radiation and chemotherapy. Annu Rev Med 66, 129–143. [PubMed: 25423595]

Goodarzi AA, and Jeggo PA (2013). The repair and signaling responses to DNA double-strand breaks. Adv Genet 82, 1–45. [PubMed: 23721719]

Gudjonsson T, Altmeyer M, Savic V, Toledo L, Dinant C, Grofte M, Bartkova J, Poulsen M, Oka Y, Bekker-Jensen S, et al. (2012). TRIP12 and UBR5 suppress spreading of chromatin ubiquitylation at damaged chromosomes. Cell 150, 697–709. [PubMed: 22884692]

Gupta A, Hunt CR, Chakraborty S, Pandita RK, Yordy J, Ramnarain DB, Horikoshi N, and Pandita TK (2014). Role of 53BP1 in the regulation of DNA double-strand break repair pathway choice. Radiat Res 181, 1–8. [PubMed: 24320053]

Harding SM, and Greenberg RA (2016). Choreographing the Double Strand Break Response: Ubiquitin and SUMO Control of Nuclear Architecture. Frontiers in genetics 7, 103. [PubMed: 27375678]

Hatakeyama S, and Nakayama KI (2003). U-box proteins as a new family of ubiquitin ligases. Biochem Biophys Res Commun 302, 635–645. [PubMed: 12646216]

Hatakeyama S, Yada M, Matsumoto M, Ishida N, and Nakayama KI (2001). U box proteins as a new family of ubiquitin-protein ligases. J Biol Chem 276, 33111–33120. [PubMed: 11435423]

Hoppe T (2005). Multiubiquitylation by E4 enzymes: 'one size' doesn't fit all. Trends Biochem Sci 30, 183–187. [PubMed: 15817394]

Huang B, Bates M, and Zhuang X (2009). Super-resolution fluorescence microscopy. Annu Rev Biochem 78, 993–1016. [PubMed: 19489737]

Johnson ES, Ma PC, Ota IM, and Varshavsky A (1995). A proteolytic pathway that recognizes ubiquitin as a degradation signal. J Biol Chem 270, 17442–17456. [PubMed: 7615550]

Kowalczykowski SC (2015). An Overview of the Molecular Mechanisms of Recombinational DNA Repair. Cold Spring Harbor perspectives in biology 7.

Lee BL, Singh A, Mark Glover JN, Hendzel MJ, and Spyracopoulos L (2017). Molecular Basis for K63-Linked Ubiquitination Processes in Double-Strand DNA Break Repair: A Focus on Kinetics and Dynamics. J Mol Biol.

Liu C, Liu W, Ye Y, and Li W (2017). Ufd2p synthesizes branched ubiquitin chains to promote the degradation of substrates modified with atypical chains. Nat Commun 8, 14274. [PubMed: 28165462]

Lombardi PM, Matunis MJ, and Wolberger C (2017). RAP80, ubiquitin and SUMO in the DNA damage response J Mol Med (Berl) 95, 799–807. [PubMed: 28681078]

Lukas J, Lukas C, and Bartek J (2011). More than just a focus: The chromatin response to DNA damage and its role in genome integrity maintenance. Nat Cell Biol 13, 1161–1169. [PubMed: 21968989]

Martin-Hernandez K, Rodriguez-Vargas JM, Schreiber V, and Dantzer F (2017). Expanding functions of ADP-ribosylation in the maintenance of genome integrity. Semin Cell Dev Biol 63, 92–101. [PubMed: 27670719]

Matsumoto M, Yada M, Hatakeyama S, Ishimoto H, Tanimura T, Tsuji S, Kakizuka A, Kitagawa M, and Nakayama KI (2004). Molecular clearance of ataxin-3 is regulated by a mammalian E4. The EMBO journal 23, 659–669. [PubMed: 14749733]

Meerang M, Ritz D, Paliwal S, Garajova Z, Bosshard M, Mailand N, Janscak P, Hubscher U, Meyer H, and Ramadan K (2011). The ubiquitin-selective segregase VCP/p97 orchestrates the response to DNA double-strand breaks. Nature cell biology 13, 1376–1382. [PubMed: 22020440]

Panier S, and Durocher D (2013). Push back to respond better: regulatory inhibition of the DNA double-strand break response. Nature reviews. Cancer 13, 661–672.

Park JY, Zhang F, and Andreassen PR (2014). PALB2: the hub of a network of tumor suppressors involved in DNA damage responses. Biochimica et biophysica acta 1846, 263–275. [PubMed: 24998779]

Park Y, Yoon SK, and Yoon JB (2008). TRIP12 functions as an E3 ubiquitin ligase of APP-BP1. Biochem Biophys Res Commun 374, 294–298. [PubMed: 18627766]

Park Y, Yoon SK, and Yoon JB (2009). The HECT domain of TRIP12 ubiquitinates substrates of the ubiquitin fusion degradation pathway. J Biol Chem 284, 1540–1549. [PubMed: 19028681]

Paull TT (2015). Mechanisms of ATM Activation. Annu Rev Biochem 84, 711–738. [PubMed: 25580527]

Pellegrino S, and Altmeyer M (2016). Interplay between Ubiquitin, SUMO, and Poly(ADP-Ribose) in the Cellular Response to Genotoxic Stress. Front Genet 7, 63. [PubMed: 27148359]

Periz G, Lu J, Zhang T, Kankel MW, Jablonski AM, Kalb R, McCampbell A, and Wang J (2015). Regulation of protein quality control by UBE4B and LSD1 through p53-mediated transcription. PLoS Biol 13, e1002114. [PubMed: 25837623]

Pierce AJ, Hu P, Han M, Ellis N, and Jasin M (2001). Ku DNA end-binding protein modulates homologous repair of double-strand breaks in mammalian cells. Genes Dev 15, 3237–3242. [PubMed: 11751629]

Pinder J, Salsman J, and Dellaire G (2015). Nuclear domain 'knock-in' screen for the evaluation and identification of small molecule enhancers of CRISPR-based genome editing. Nucleic Acids Res 43, 9379–9392. [PubMed: 26429972]

Polo SE, and Jackson SP (2011). Dynamics of DNA damage response proteins at DNA breaks: a focus on protein modifications. Genes Dev 25, 409–433. [PubMed: 21363960]

Poulsen M, Lukas C, Lukas J, Bekker-Jensen S, and Mailand N (2012). Human RNF169 is a negative regulator of the ubiquitin-dependent response to DNA double-strand breaks. J Cell Biol 197, 189–199. [PubMed: 22492721]

Ramadan K (2012). p97/VCP- and Lys48-linked polyubiquitination form a new signaling pathway in DNA damage response. Cell Cycle 11, 1062–1069. [PubMed: 22391235]

Reid DA, Keegan S, Leo-Macias A, Watanabe G, Strande NT, Chang HH, Oksuz BA, Fenyo D, Lieber MR, Ramsden DA, et al. (2015). Organization and dynamics of the nonhomologous end-joining machinery during DNA double-strand break repair. Proc Natl Acad Sci U S A 112, E2575–2584. [PubMed: 25941401]

Saeki Y, Tayama Y, Toh-e A, and Yokosawa H (2004). Definitive evidence for Ufd2-catalyzed elongation of the ubiquitin chain through Lys48 linkage. Biochem Biophys Res Commun 320, 840–845. [PubMed: 15240124]

Segal-Raz H, Mass G, Baranes-Bachar K, Lerenthal Y, Wang SY, Chung YM, Ziv-Lehrman S, Strom CE, Helleday T, Hu MC, et al. (2011). ATM-mediated phosphorylation of polynucleotide kinase/phosphatase is required for effective DNA double-strand break repair. EMBO Rep 12, 713–719. [PubMed: 21637298]

Shibata A, and Jeggo PA (2014). DNA double-strand break repair in a cellular context. Clinical oncology 26, 243–249. [PubMed: 24630811]

Shiloh Y, and Ziv Y (2013a). The ATM protein kinase: regulating the cellular response to genotoxic stress, and more. Nat Rev Mol Cell Biol 14, 197–210.

Shiloh Y, and Ziv Y (2013b). The ATM protein kinase: regulating the cellular response to genotoxic stress, and more. Nat Rev Mol Cell Biol.

Sims JJ, Scavone F, Cooper EM, Kane LA, Youle RJ, Boeke JD, and Cohen RE (2012). Polyubiquitin-sensor proteins reveal localization and linkage-type dependence of cellular ubiquitin signaling. Nat Methods 9, 303–309. [PubMed: 22306808]

Sirbu BM, and Cortez D (2013). DNA damage response: three levels of DNA repair regulation. Cold Spring Harbor perspectives in biology 5, a012724.

Spasser L, and Brik A (2012). Chemistry and biology of the ubiquitin signal. Angew Chem Int Ed Engl 51, 6840–6862. [PubMed: 22696461]

Starita LM, Pruneda JN, Lo RS, Fowler DM, Kim HJ, Hiatt JB, Shendure J, Brzovic PS, Fields S, and Klevit RE (2013). Activity-enhancing mutations in an E3 ubiquitin ligase identified by high-throughput mutagenesis. Proc Natl Acad Sci U S A 110, E1263–1272. [PubMed: 23509263]

Sun Y, Jia X, Gao Q, Liu X, and Hou L (2017). The ubiquitin ligase UBE4A inhibits prostate cancer progression by targeting interleukin-like EMT inducer (ILEI). IUBMB Life 69, 16–21. [PubMed: 27862841]

Symington LS (2016). Mechanism and regulation of DNA end resection in eukaryotes. Critical reviews in biochemistry and molecular biology 51, 195–212. [PubMed: 27098756]

Thorslund T, Ripplinger A, Hoffmann S, Wild T, Uckelmann M, Villumsen B, Narita T, Sixma TK, Choudhary C, Bekker-Jensen S, et al. (2015). Histone H1 couples initiation and amplification of ubiquitin signalling after DNA damage. Nature 527, 389–393. [PubMed: 26503038]

Torrecilla I, Oehler J, and Ramadan K (2017). The role of ubiquitin-dependent segregase p97 (VCP or Cdc48) in chromatin dynamics after DNA double strand breaks. Philos Trans R Soc Lond B Biol Sci 372.

Typas D, Luijsterburg MS, Wiegant WW, Diakatou M, Helfricht A, Thijssen PE, van den Broek B, Mullenders LH, and van Attikum H (2015). The deubiquitylating enzymes USP26 and USP37 regulate homologous recombination by counteracting RAP80. Nucleic acids research 43, 6919–6933. [PubMed: 26101254]

van de Linde S, Loschberger A, Klein T, Heidbreder M, Wolter S, Heilemann M, and Sauer M (2011). Direct stochastic optical reconstruction microscopy with standard fluorescent probes. Nat Protoc 6, 991–1009. [PubMed: 21720313]

Villarreal DD, Lee K, Deem A, Shim EY, Malkova A, and Lee SE (2012). Microhomology directs diverse DNA break repair pathways and chromosomal translocations. PLoS genetics 8, e1003026. [PubMed: 23144625]

Wani AH, Boettiger AN, Schorderet P, Ergun A, Munger C, Sadreyev RI, Zhuang X, Kingston RE, and Francis NJ (2016). Chromatin topology is coupled to Polycomb group protein subnuclear organization. Nat Commun 7, 10291. [PubMed: 26759081]

Williamson A, Werner A, and Rape M (2013). The Colossus of ubiquitylation: decrypting a cellular code. Mol Cell 49, 591–600. [PubMed: 23438855]

Wilson MD, and Durocher D (2017). Reading chromatin signatures after DNA double-strand breaks. Philos Trans R Soc Lond B Biol Sci 372.

Wu H, and Leng RP (2011). UBE4B, a ubiquitin chain assembly factor, is required for MDM2-mediated p53 polyubiquitination and degradation. Cell Cycle 10, 1912–1915. [PubMed: 21558803]

Wu H, Pomeroy SL, Ferreira M, Teider N, Mariani J, Nakayama KI, Hatakeyama S, Tron VA, Saltibus LF, Spyracopoulos L, et al. (2011). UBE4B promotes Hdm2-mediated degradation of the tumor suppressor p53. Nat Med 17, 347–355. [PubMed: 21317885]

Yokoi M, and Hanaoka F (2017). Two mammalian homologs of yeast Rad23, HR23A and HR23B, as multifunctional proteins. Gene 597, 1–9. [PubMed: 27771451]

Young LM, Marzio A, Perez-Duran P, Reid DA, Meredith DN, Roberti D, Star A, Rothenberg E, Ueberheide B, and Pagano M (2015). TIMELESS Forms a Complex with PARP1 Distinct from Its Complex with TIPIN and Plays a Role in the DNA Damage Response. Cell Rep 13, 451–459. [PubMed: 26456830]

Yun MH, and Hiom K (2009). CtIP-BRCA1 modulates the choice of DNA double-strand-break repair pathway throughout the cell cycle. Nature 459, 460–463. [PubMed: 19357644]

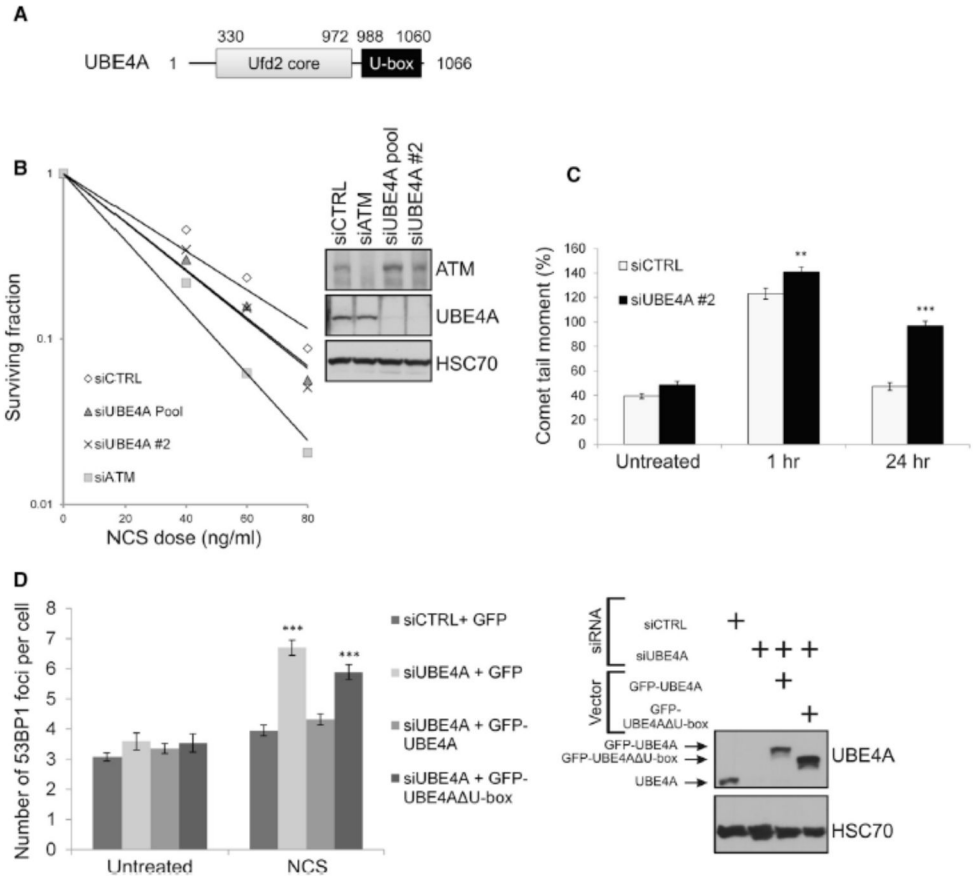

1. UBE4A depletion affects DSB repair.

(A) Domain diagram of UBE4A. **(B)** UBE4A depletion leads to cellular hypersensitivity to the radiomimetic chemical, NCS. Clonogenic survival curves of CAL51 cells transfected with control siRNA (siCTRL) or two siRNAs directed against UBE4A and subsequently treated with various NCS doses. siCTRL cells and cells transfected with siATM served as controls. The immunoblot shows the degree of protein depletion for UBE4A and ATM. **(C)** Direct observation of DSBs in UBE4A-proficient and depleted A549 cells using a neutral comet assay, 1 and 24 hr after irradiation with 10 Gy of IR. **(D)** Numbers of 53BP1 nuclear foci in cells 24 hr after treatment with 20 ng/ml of NCS. Cells were transfected with the indicated siRNAs and with vectors expressing GFP or siRNA-resistant cDNAs encoding GFP-tagged wild-type UBE4A or mutant UBE4A lacking the U-box (GFP-UBE4AΔU-box). The immunoblot shows the extents of endogenous UBE4A depletion and expression of ectopic proteins.

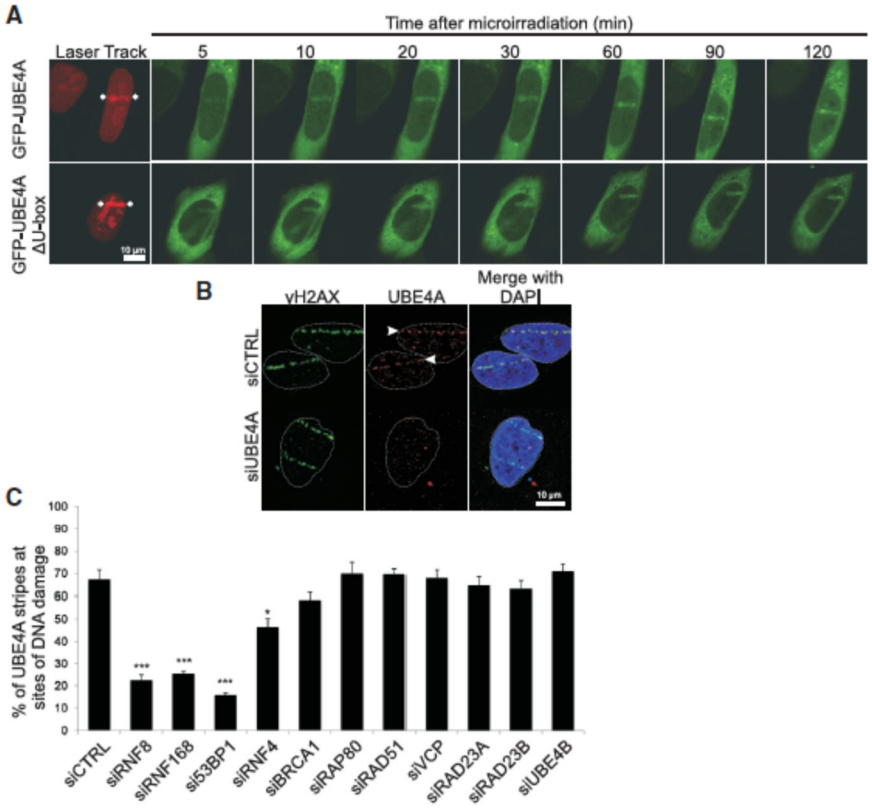

Figure 2. UBE4A relocalizes to sites of DNA damage dependent upon other E3 ligases and 53BP1.

(A) Dynamics of UBE4A relocalization to damage sites in live cells. Cells were depleted of endogenous UBE4A using RNAi and co-transfected with vectors expressing siRNA-resistant cDNAs of GFP-UBE4A or GFP-UBE4AΔU-box, together with DsRed2-tagged polynucleotide kinase-phosphatase (PNKP). The rapid recruitment of PNKP to damage sites (red) (Segal-Raz et al., 2011) marks their location. Localized DNA damage was induced using a focused laser microbeam and the cells were monitored by time-lapse imaging. Note the rapid recruitment to laser-induced damage sites of both wild-type and mutant UBE4A (green). **(B)** Recruitment of endogenous UBE4A to sites of laser-induced damage. Cells were transfected with siRNA against UBE4A or irrelevant siRNA, treated with laser microirradiation, and immunostained 40 min later with antibodies against UBE4A and γH2AX. **(C)** Using the same experimental setup as in **(B)**, the cells were transfected with the indicated siRNAs, treated with laser microirradiation, and monitored for recruitment of endogenous UBE4A to damage sites 20 min later. The fraction of γH2AX stripes co-stained for UBE4A was recorded and is presented in the upper panel as mean ± SD (3 independent experiments, n=200). *p<0.05, ***p<0.0005 (student's t-test). (See also Figure S2).

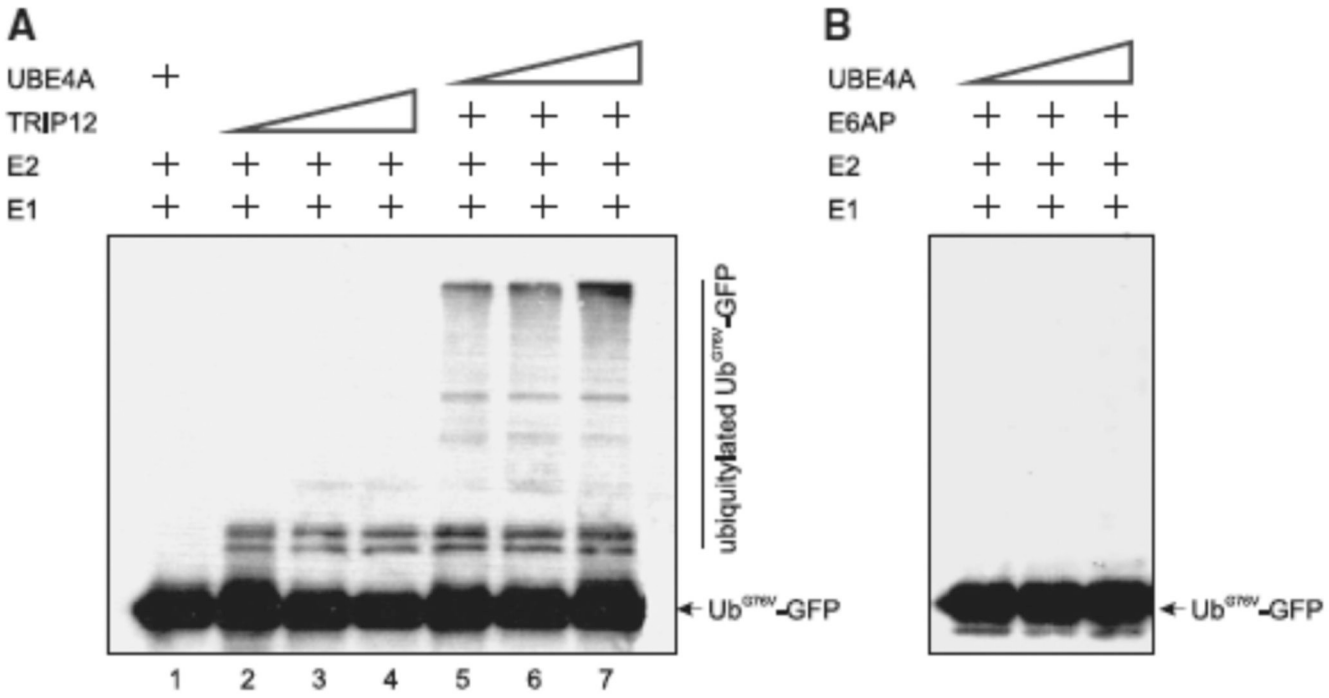

Figure 3. E4 ligase activity of UBE4A *in vitro*.

(A) His6-Ub^{G76V}-GFP (300 ng) was incubated for 1h at 37 °C with FLAG-TRIP12 (200 and 400 ng in lanes 2 and 3, respectively, and 800 ng in lanes 4-6) and FLAG-UBE4A (250 and 500 ng in lanes 5 and 6, respectively, and 1000 ng in lanes 1 and 7) in a reaction mixture containing 2 mM ATP, 800 ng of His6-Ub, 100 ng of His6-Uba1, 250 ng of His6-UbcH5a. The reaction was terminated by addition of 2X Laemmli sample buffer and subjected to SDS-PAGE. The blot was subsequently probed with an anti-GFP antibody. **(B)** Similar reactions as in (A) with another E3 ligase, E6AP, replacing TRIP12. (See also Figure S4).

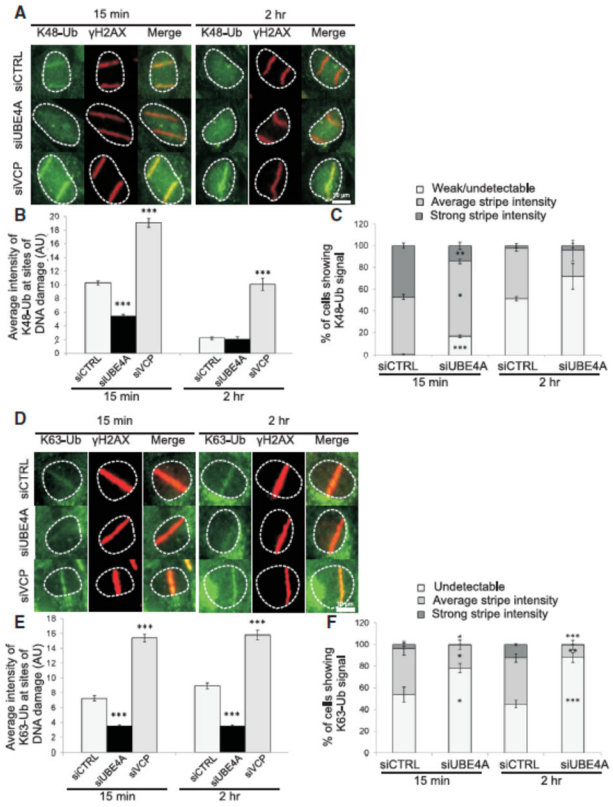

Figure 4. UBE4A is required for timely and quantitatively proper assembly of ubiquitin chains at sites of DNA damage.

(A) Cells were transfected with the indicated siRNAs, and localized DNA damage was induced using a focused laser microbeam. The cells were fixed 15 min or 2 hr later and stained with antibodies against γH2AX and K48-Ub. **(B)** The accumulation of K48-Ub was quantified according to the fluorescence intensity obtained using the corresponding antibody on top of γH2AX stripes. The immunoblot shows the extent of UBE4A depletion in tis experiment. **(C)** K48-Ub lines were classified as 'strong', 'average' or 'weak/undetectable'. **(D-F)** Similar analysis as in (A-C) for K63-linked ubiquitin chains. AU - arbitrary units. Quantified data in B and C are represented as mean ± SEM (3 independent experiments, n>70), and in E and F as mean ± SEM (4 independent experiments, n>80). *p<0.05, ** p<0.005, *** p-<0.0005 (student's t-test, relative to the siCTRL). (See also Figures S6 and S7).

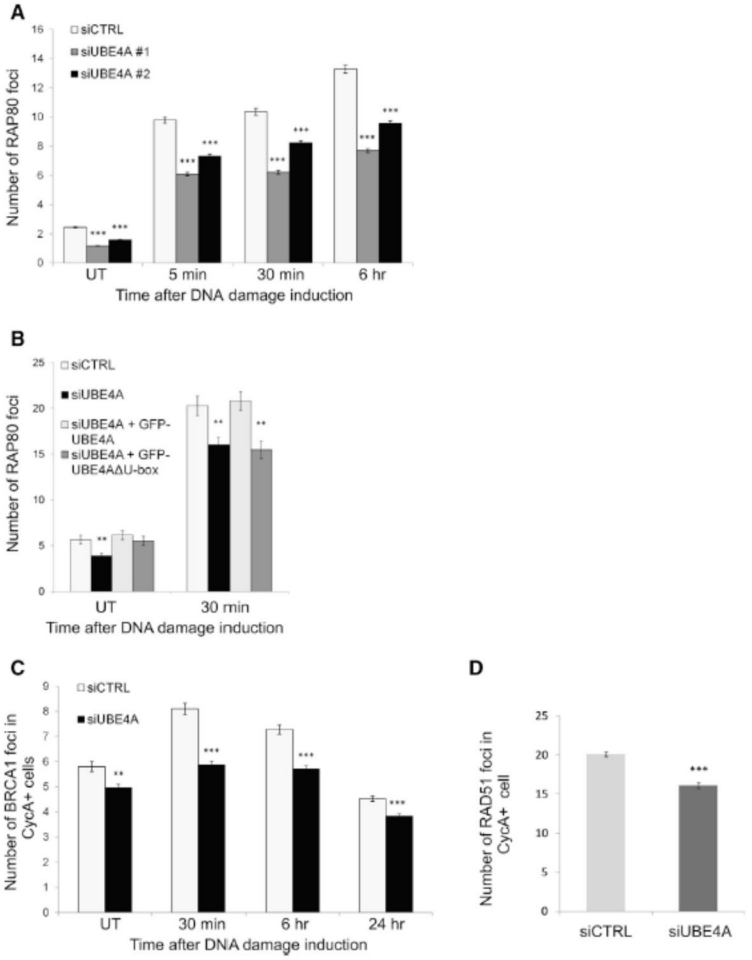

Figure 5. UBE4A is required for assembly of ubiquitin-dependent factors at sites of DNA damage, in a U-box-dependent manner.

(A) U2-OS cells were transfected with the indicated siRNA, treated with 20 ng/ml of NCS, and stained for nuclear foci of RAP80 at the indicated time points. **(B)** U2-OS cells were transfected with irrelevant or siRNA against UBE4A, as well as constructs expressing siRNA-resistant wild-type GFP-UBE4A or GFP-UBE4A(ΔU-box). 48 hr later the cells were treated with 20 ng/ml of NCS and stained for nuclear foci of RAP80. **(C)** U2-OS cell were transfected with the indicated siRNA, treated with 20 ng/ml of NCS, and stained for nuclear foci of BRCA1 and cyclin-A2 at the indicated time points. BRCA1 foci were quantified in cyclin-A2-positive cells (i.e., cells at the S and G2 phases of the cell cycle). **(D)** U2-OS cell transfected with the indicated siRNA, treated with 1 Gy of IR, and 1 hr later stained for RAD51 and cyclin A2. Shown are percentages of cyclin A2-positive cells with more than 10 RAD51 foci/cell. Quantified data represented as mean ± SEM (2 independent experiments, n>100, except in (E) where mean ± SD is shown (3 independent experiments, n>600). *p<0.05. ***p<0.0001 (student's t-test). UT: untreated. Images in (A) and (C) were captured and analyzed using the Hermes WIScan apparatus. Images in (B) were captured using conventional fluorescence microscopy and analyzed using ImageJ software. Quantified data are presented as mean ± SEM [2 independent experiments, n>2000, in (A) and (C), and 2

independent experiments, n=100 in (B)]. **p<0.005, ***p<0.0005 (student's t-test, relative to the siCTRL).

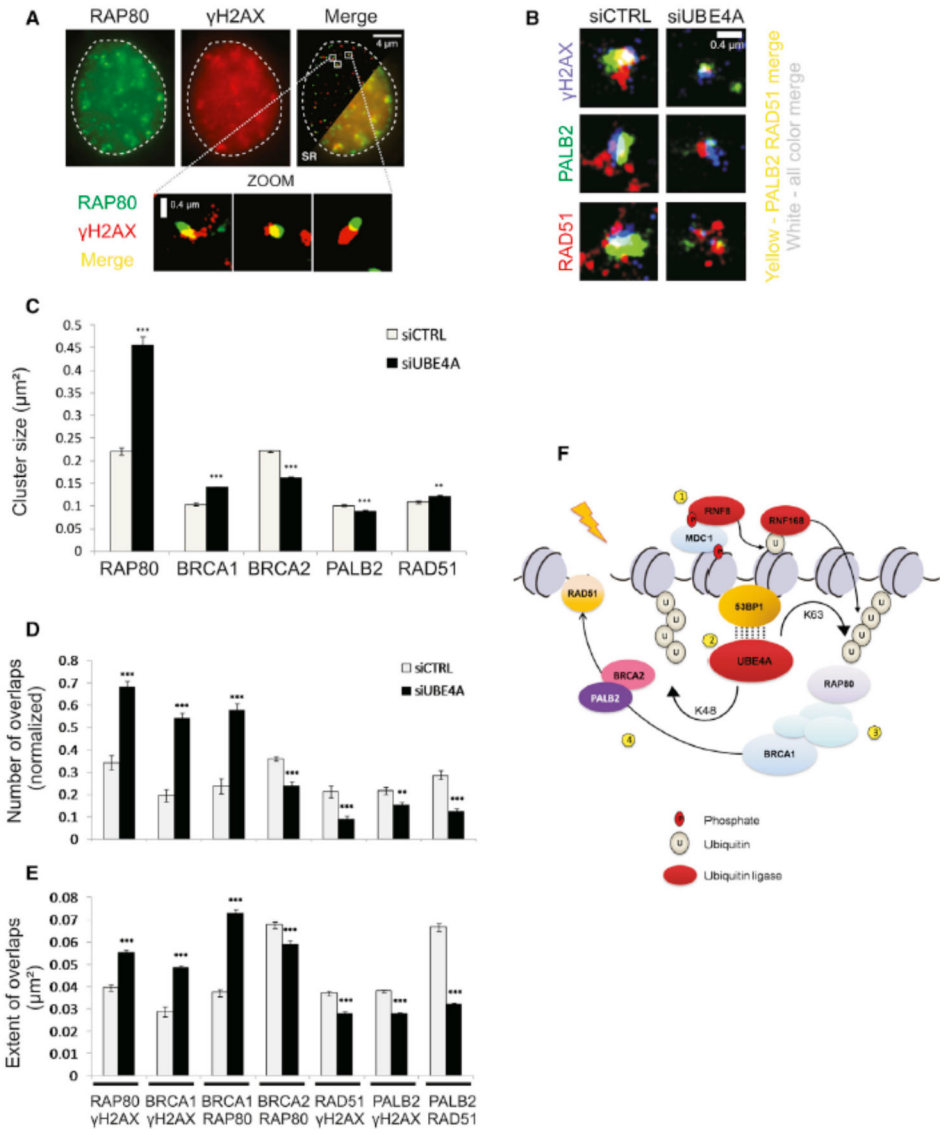

Figure 6. UBE4A affects focus organization at sites of DNA damage.

(A) Conventional diffraction limited total internal reflection fluorescence (TIRF) microscope image of γH2AX and RAP80. Merged image with cutaway super-resolution (SR) revealing the improved resolution. Lower panel: Selected zoomed regions showing γH2AX/RAP80 foci. **(B)** Representative image of the overlaps of RAD51/PALB2/γH2AX foci particles in cells treated with control or UBE4A siRNAs and treated with NCS for 30 min. **(C)** Quantification of the average area of focus particles (denoted as 'cluster size') of various DDR proteins in cells treated with control or UBE4A siRNA and subsequently treated with NCS for 30 min. **(D)** Quantification of the number of overlaps per nucleus (normalized to the total number of particles detected) between different pairs of DDR factors. **(E)** Quantification of the extent of overlap between various DDR factors in cells treated with control or UBE4A siRNA and subsequently treated with NCS for 30 min. **(F)** Molecular model for the role of UBE4A in ubiquitin signal enhancement. (1) The ubiquitin E3 ligases, RNF8 and RNF168, are recruited to DSB sites and mediate protein ubiquitylation. (2)

UBE4A is recruited in a 53BP1-dependent manner and regulates further adjustment of K48- and K63-linked ubiquitin chains. The dotted lines indicate physical interaction that may be mediated by other proteins. (3) RAP80 is recruited to K63-Ub, thereby recruiting BRCA1 to form the BRCA1-A complex. (4) UBE4A promotes the dynamic reorganization of the BRCA1-A complex into the BRCC complex, which in turn promotes RAD51 recruitment and HRR. (See also Figure S8).

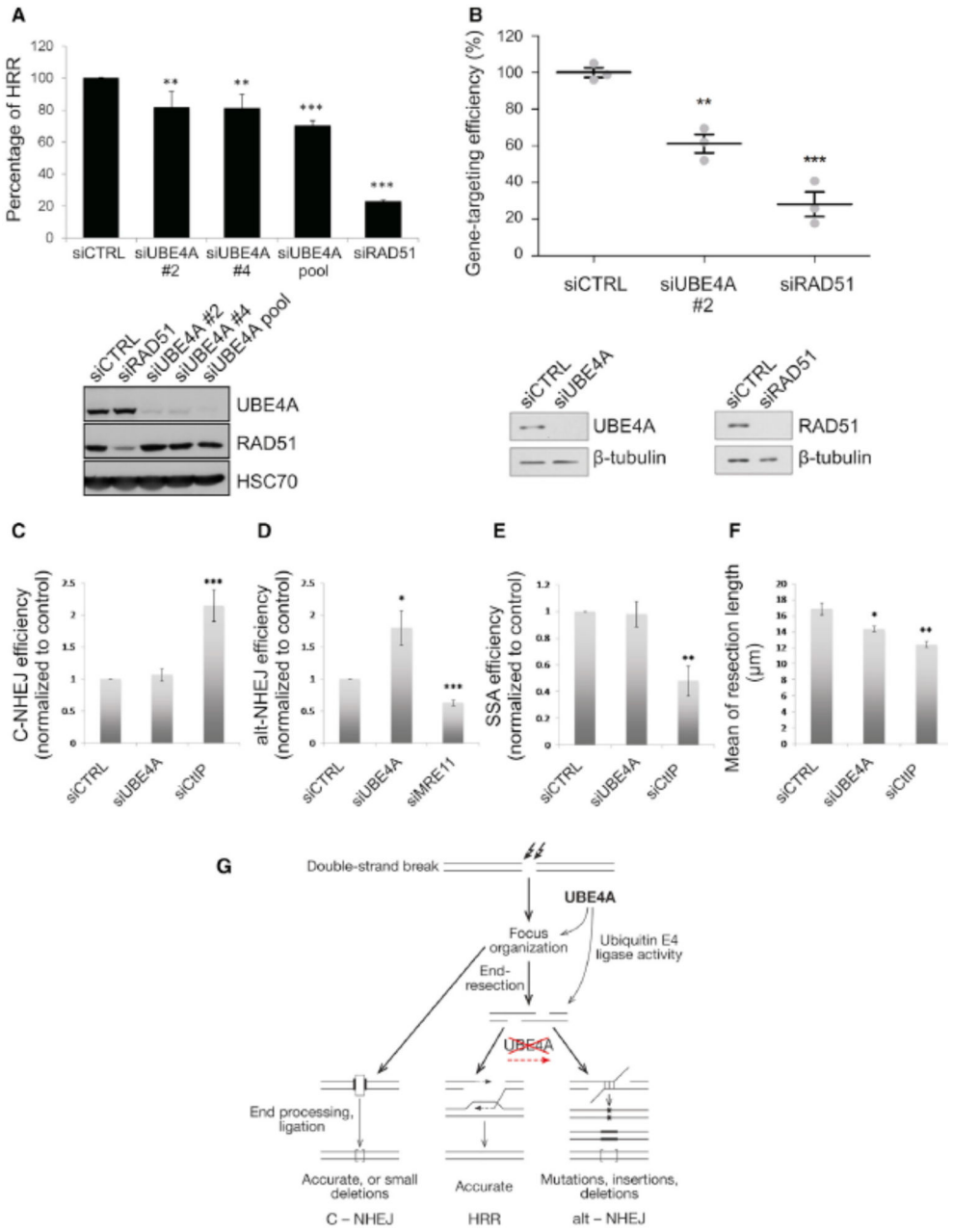

Figure 7. UBE4A depletion interferes with the balance between DSB repair pathways.

(A) HRR measurement based on the DR-GFP assay (Pierce et al., 2001). The siUBE4A pool includes four siRNA sequences: siRNAs #1 to siRNA #4. Cells transfected with irrelevant siRNA or siRNA against RAD51 – a major HRR protein – served as controls. **(B)** CRISPR-mediated HDR. The CRISPR clover-LMNA HDR assay (Pinder et al., 2015) was conducted in U2-OS cells in triplicate (n= 500-750 cells per replicate) and error bars = SEM. **p<0.03, ***p<0.001 (Student's t-test). The blots show the extent of protein depletion in this experiment. (See also Figure S7). **(C-E)** C-NHEJ, alt-NHEJ and SSA measured using the EJ5-GFP, EJ2-GFP and SA-GFP reporters (Bennardo et al., 2008), respectively. In all cases, repair of an I-SceI meganuclease-induced DSB renders the cells GFP positive when repair is

achieved via the indicated pathway. The efficiency of repair was calculated as the percentage of GFP positive cells in response to I-SceI expression upon downregulation of the indicated genes, normalized against the control. The average and standard deviation of at least three independent experiments is shown. **(F)** End-resection measured using the SMART assay (Cruz-Garcia et al., 2014). Median resection length was measured one hour after exposing cells transfected with the indicated siRNAs to 10 Gy of IR. The average and standard deviation of four independent experiments is shown. For each replica, at least 300 individual ssDNA fibers were measured. *$p<0.05$, **$p<0.005$. **(G)** A model scheme showing the role of UBE4A-mediated modulation of protein ubiquitylation in pathway choice during DSB repair.